

# Differentiation in a globally coupled circle map with growth and death

F.H. Willeboordse<sup>a</sup>

Dept. of Physics, The National University of Singapore, Singapore 119260

Received 29 April 2004 / Received in final form 6 January 2005

Published online 8 August 2005 – © EDP Sciences, Società Italiana di Fisica, Springer-Verlag 2005

**Abstract.** A key characteristic of biological systems is the continuous life cycle where cells are born, grow and die. From a dynamical point of view the events of cell division and cell death are of paramount importance and constitute a radical departure from systems with a fixed size. In this paper, a globally coupled circle map where elements can dynamically be added and removed is investigated for the conditions under which differentiation of roles can occur. In the presence of an external source, it is found that populations of very long-living cells are sustained by short-living cells. In the case without an external source, it is found that at higher nonlinearities of the local map, large populations cannot be sustained with a previously employed division strategy but that a different and conceptually equally natural division strategy allows for differentiation of roles.

**PACS.** 05.45.Ra Coupled map lattices

## 1 Introduction

Coupled Map Lattices have widely been studied as simple and efficient paradigms for the complex dynamics of higher dimensional systems in e.g. Mathematics, Physics and Chemistry. Generally, the investigated models covering these fields are characterized by a fixed system size where the coupling can be local [1–7], global [8–11] or intermediate [12–15]. Although the range of observed phenomena in these systems is extremely wide, they do lack one essential aspect that is of paramount importance to the study of biological networks: The dynamical addition and removal of elements. Since ordinary coupled map lattices have proven to be very valuable tools, it is sensible to attempt an extension of that approach despite the fact that biological systems are usually vastly more complex than the systems commonly studied in Physics and Chemistry. The relevance of this idea was strikingly illustrated by Ko and coworkers who found that the dynamical state of E.Coli bacteria (in the absence of mutations) is not determined entirely by its environment and its genome as often believed, but that even with an identical genome and in an identical environment, cells with different phenotypes can emerge [16]. Indeed, the notion that cells with identical genotype can express themselves differently depending on their state underlies experimental studies where phenotypic behaviors mimic logical operations leading to the cells performing controllable

computations like e.g. a genetic toggle switch [17–20]. These phenomena are reminiscent of the clustering described by Kaneko for globally coupled logistic maps [8] and a basis for Kaneko and Yomo’s isologous diversification theory [21] which was introduced as a framework for understanding cell differentiation from the viewpoint of complex systems. Even though compared to the actual chemical reactions occurring in a cell, the model equations of the isologous diversification theory are a vast simplification, being differential in nature, they are still significantly too complicated to serve as a true toy model. Kaneko therefore introduced the coupled map with growth and death studied in this paper in order to have a simple system for investigating possible dynamics [22].

This paper is organized as follows: in Section 2, Kaneko’s model as introduced in reference [22] is outlined and his main results are briefly summarized. It is argued that it is of interest to consider other values of a key parameter, the source term  $s$ , besides the single fixed non-zero value investigated in reference [22] and that the dynamics display distinct features for  $s = 0$  and for  $s$  larger or smaller than a critical value  $s_c$  (Kaneko’s value of  $s$  is above  $s_c$ ). The dynamics of the system for  $s > s_c$  is described in Section 3 and extends Kaneko’s results by considering long simulation times that can lead to populations of long-living cells while the dynamics for  $s < s_c$  is described in Section 4 and studied here for the first time. Sections 5 and 6 investigate the dependence of the system on parameter settings and division-mutation strategies respectively that were not considered before and show that

<sup>a</sup> e-mail: willeboordse@yahoo.com;  
URL: <http://www.willeboordse.ch/science/>

co-existing long and short-living cells can exist for a certain division strategy. A conclusion with a brief discussion of the results is presented in Section 7.

## 2 Model

The coupled map with growth and death Kaneko introduced in reference [22] consists of elements with oscillatory internal dynamics, called cells for convenience and is given by

$$x_{n+1}^i = x_n^i + f(x_n^i) + S_n, \quad (1)$$

$$S_n = \frac{s - \sum_j f(x_n^j)}{N}, \quad (2)$$

with  $n$  the discrete time,  $i$  an index uniquely identifying a cell,  $S_n$  a source term and  $N$  the total number of cells. The source term  $S_n$  is designed such that the sums of the cells before and after applying equation (1) exactly differ by the externally supplied amount  $s$ . The oscillatory nature of the cell's internal state is represented by choosing the circle map

$$f(x) = \frac{K}{2\pi} \sin(2\pi x) \quad (3)$$

as the non-linear local map where the parameter  $K$  determines the nonlinearity which ranges from zero to  $2\pi$ . The Feigenbaum accumulations point, the smallest value of  $K$  where chaos is possible here, is around  $K = 2.72$  and there is large window from around  $K = 4.6$  to  $K = 5.26$ . The local dynamics only depend on the phase or in other words the fractional part of  $x^i$ . The conditions for the splitting or death of a cell are:

- A cell splits if  $x > T_g$  with  $T_g = 10$
- A cell dies if  $x < T_d$  with  $T_d = 0$ .

The exact values for  $T_g$  and  $T_d$  are generally not important for the qualitative aspects of the *local* dynamics as long as they are integer values since equation (1) is period 1. Nevertheless, if  $T_g - T_d$  is an integer value somewhat larger than 1, cells can change their winding number (the integer part of  $x$ ) before stabilizing and thus the existence of several different winding numbers can play an important role for the *global* dynamics. Except when mentioned otherwise, upon splitting, the two daughter cells each receive half of the parents cell's fractional part. Furthermore a small random number  $\delta$  (here  $10^{-9}$  is used) is added to one daughter cell and subtracted from the other daughter cell in order to introduce a slight difference between the new cells.

Overall, equation (1) is a type of globally coupled map [8]. Globally coupled maps have widely been studied and are often characterized by the dynamics of their clusters which are defined as follows: When two elements  $x^i$  are very close, i.e.  $|x^i - x^j| < \epsilon$  with  $\epsilon$  a small number (in this paper  $\epsilon = 10^{-5}$  is used), they are considered to belong to the same cluster. An attractor can in principle consist of any number of clusters ranging from a single large cluster to  $N$  one-element clusters. Following [8], the

clusters of an attractor are labeled as  $N_1, N_2, \dots, N_k$  in order of size with  $N_1$  being the largest cluster and  $k$  the total number of clusters (consequently  $\sum_{j=0}^k N_j = N$ ). Based on cluster arrangement, four phases are well-known to be common among globally coupled maps: 1) Coherent phase where  $N_1 = N$  is dominant, 2) Ordered phase where  $k$  is relatively small and independent of  $N$ , 3) Partially ordered phase where ordered-phase type few cluster attractors coexist with large- $k$  many-cluster attractors (for many-cluster attractors  $k$  is dependent on  $N$ ), 4) Turbulent phase where  $k \approx N$ .

Similarly, the dynamics of equation (1) can be classified by four main phases that occur when increasing the nonlinearity  $K$ :

- 1) *Coherent phase* where all the elements are part of a single cluster,
- 2) *Ordered Phase* where elements tend to be synchronized into a few clusters,
- 3) *Partially Ordered Phase* where the elements can dynamically join and leave a cluster, and
- 4) *Desynchronized Phase* where the elements' oscillations are usually desynchronized<sup>1</sup>.

Although the four phases of the model with growth and death share many features in common with the four phases of a fixed system-size globally coupled map, there are also essential differences. For example, during the rather long transient of the partially ordered phase there are two separate temporal regimes, one in which the total number of cells fluctuates around  $O(10)$  and one where the total number of cells grows to  $O(100)$ , whereas in the desynchronized phase the total number of cells after some transient time is limited to  $O(10)$  regardless of the initial number of cells.

While mostly, for the overall behavior of the system, the exact value of the global source term  $s$  in equation (1) is not very important, there are nevertheless three distinctive regimes. Firstly, there is a distinction of whether there is a global source at all. Without a source, the dynamics is entirely determined by the interaction of the elements. If there is a source, however, even when it is very small, cells have an intrinsic tendency to grow and thus have some sort of life cycle. When increasing the source from 0, the qualitative dynamics of the system does not change smoothly. Rather, it turns out that there is a critical value for the source  $s_c$  below which the population is mostly 1 and above which population growth and more complex dynamics are possible. This critical source is depicted in Figure 1 and was determined as the source value at which the ratio of a single cell population to a multi cell population is 0.5 over a time span of one million time steps after a transient of half a million time steps.

The main effect of further increasing  $s$  above  $s_c$  is an increase of the average population.

<sup>1</sup> Since the coherent phase in a strict sense does not exist when  $s \neq 0$ , it is not mentioned in [22] giving rise to only three main phases.

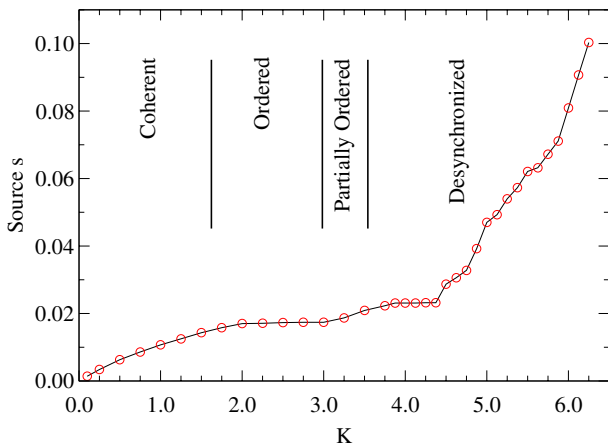


**Fig. 1.** The critical value of the source  $s_c$  below which the population is mostly 1 and above which population growth can occur.

### 3 Sources greater than $s_c$

When the source term  $s$  is greater than  $s_c$ , the population is generally larger than  $N = 1$  for any value of  $K > 0$ . For very small  $K$ , roughly in the range from 0 to 1.6, the system is mostly coherent with a single cluster as can be seen in Figure 2a. Then, roughly for  $K$  ranging from 1.6 to 3.0, the system is in the ordered phase of which an example is given in Figure 2c.

When increasing  $K$ , the disorder generated by cell division increases to the point where (some) cells can grow up to the division point  $T_g$  without joining a cluster. This happens roughly for  $K = 3.0$  and marks the start of the partially ordered phase where cluster numbers can range from 1 to  $N$ . For smaller nonlinearities in this phase (i.e. for  $K \approx 3.1$ ), there is a (very) long transient during which cells grow and divide giving rise to an increasing population until at some stage the source term becomes insufficient to support rapid growth in the  $x$ -values of the cells. The slower growth allows the cells to be attracted to a single cluster which will then grow and divide. Upon division, however, most of the newborn cells do not survive and the population collapses after which the cycle starts over again [22]. This is shown in Figure 3a with the corresponding population strip chart in b).

After the transient, long-living clusters can emerge. These coexist with (a smaller number of) non-clustered cells. While the  $x$ -values of these clusters fluctuate around some level, their size increases gradually by the joining of non-clustered cells. Generally, this joining of non-clustered cells does not affect the average population size of the non-clustered cells which grow and divide rapidly. At some stage, however, as the amount of source  $s$  per cell decreases with the increasing overall population size, a single coherent cluster may still emerge which will grow until  $T_g$  is reached. As is the case for smaller  $K$ , upon cell division of a single large cluster, oftentimes most of the new cells die rapidly and the population collapses. This situation is depicted in Figure 3c where the long-living clusters are

drawn with a thick line with the corresponding population strip chart given in d).

Towards the end of the partially ordered phase, from around  $K \approx 3.3$ , after a transient of  $10^6$  to  $10^7$  time steps with dynamics similar to the one described in the preceding paragraph, a rather stable system of co-existing long- and short-living cells emerges. Figure 4a shows the state of the system after 62 million time steps. The population at this point in time fluctuates around 2087 cells in the cluster represented by the upper thick line and 746 cells in the cluster represented by the lower thick line. While, by inspecting the ages of the cells in the clusters, it is clear that cells keep on joining the clusters occasionally, what is notable is that about half of all the cells are older than 50 million time steps (divided in a roughly 2:1 ration over the two large clusters). This indicates that population collapses have not occurred during this time and that the system is very stable (it is of course possible that the population will eventually collapse, however, this was not observed in several runs of  $10^8$  time steps). A key factor may be the relative sizes of the long-living clusters which were found to be in a ratio of roughly 1:2. Other ratios did not seem to survive very long. Note that in reference [22] only relatively short simulation times were investigated and that hence the emergence of the stable populations described here was not observed. The co-existence of long-living cells can be found from around  $K \approx 3.3$  to  $K \approx 3.45$  (see also Fig. 7) with a decrease of the average population size for increasing  $K$ .

It is found that the dynamics of the system is sustained by the co-existence of the short-living cells. At the time point indicated by the arrow in Figure 4c, the nonlinearity of the short-living cells was manually set to  $K = 0$ . Within 1000 time steps this led to the extinction of this group of cells after which the two large clusters merged into a single coherent cluster. As previously, once this cluster divided, most of the cells died and the population collapsed as can clearly be seen in Figure 4d.

The dynamical differences between the regimes can also be seen when considering the population histograms depicted in Figure 5. In the coherent phase shown in Figure 5a, the population fluctuates around a fixed value (in this case  $N = 12$ ). In this phase, when the cells split, all the daughter cells may survive for a short time leading to a brief doubling of the population size. This is reflected in a minor peak in the histogram (in this case  $N = 24$ ). However, some daughter cells will then die rapidly restoring the population to its preferred size (in this case  $N = 12$ ). In the ordered phase, populations can grow larger but collapse at some stage as can be inferred from Figure 5b. The coexistence of long and short living cells in the partially ordered phase leads to a steadily increasing population and hence the population histogram remains roughly flat in Figure 5c (Although the population size steadily increases, when a large cluster splits, a sudden jump in the population size is possible leading to the type of gap visible around  $N = 43000$ ). As can be expected, the histogram for the desynchronized phase is bell-curve like as

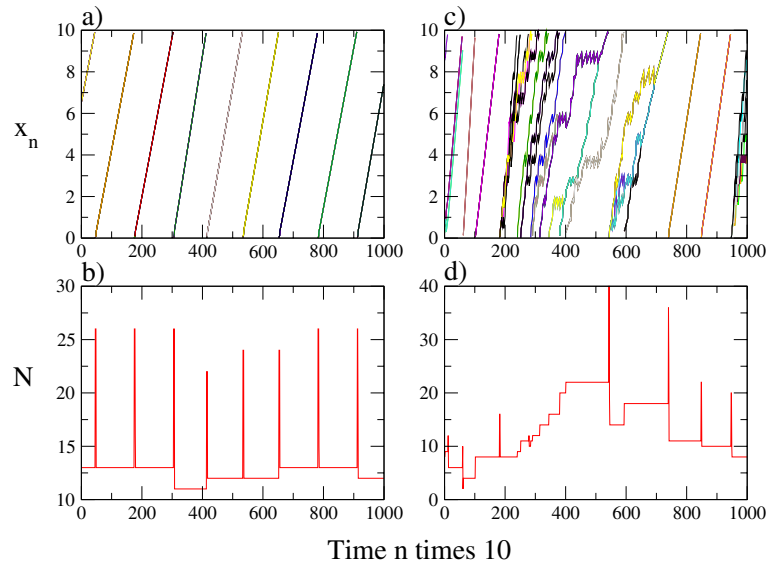


**Fig. 2.** Ordered phase after a transient of  $10^5$  time steps. The nonlinearity  $K$  is set to 1.0 in a) and b) which are nearly coherent except for a short time span after the cell divisions. In c) and d),  $K$  is set to 2.0. Graphs a) and c) depict the temporal evolution of the individual cells  $x$ -values while b) and d) show the corresponding population strip charts.  $10^5$  time steps were discarded as transients and the source was set to  $s = 0.1$ .

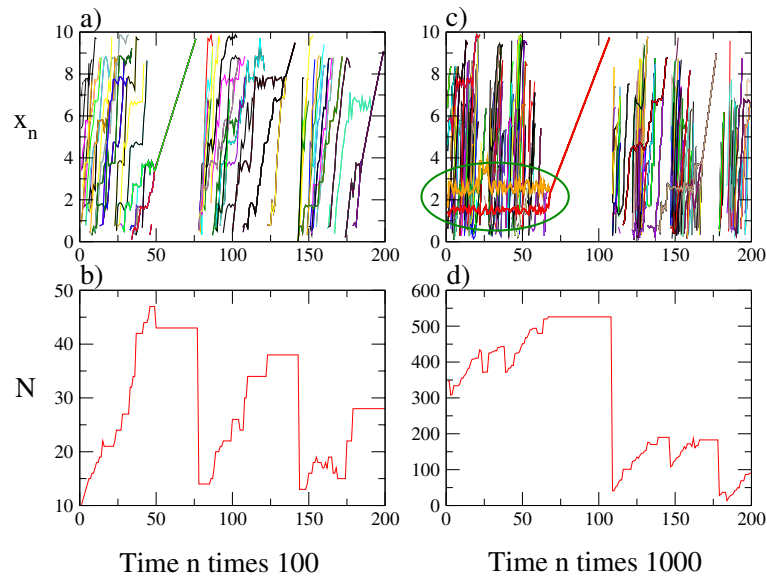


**Fig. 3.** Partially Ordered Phase with and without long-living cell clusters. In a) and b), the nonlinearity was set to  $K = 3.1$  while in c) and d) it was set to  $K = 3.2$ . In a) the situation during the long transient when there are no long-living cell clusters is depicted. In c), long-living cell clusters are indicated by the thicker lines. These clusters show no overall growth for long periods of time as can be seen by inspecting the area inside the ellipse.  $10^6$  time steps were discarded as transients and the source was set to  $s = 0.1$ . Graphs b) and d) are the population strip charts corresponding to graphs a) and c) respectively.

can be seen in Figure 5d. Age distributions corresponding to Figures 4a and 5c are shown in Figure 6. The peak in Figure 6a corresponds to the splitting of a large cluster which led to particularly many cells to be attracted to a long-living cluster, while the peak in Figure 6b corresponds to the cells which formed the initial long-living cluster. The fact that remaining data points are greater than zero (i.e. that there are cells of all ages) indicates the gradual attraction of cells to one of the clusters.

Near the transition from the partially ordered to the desynchronized phase, the coexistence of short- and

long-living cells can also occur for relatively small populations as compared to the situation depicted in Figure 4. Figure 7 shows the system after  $1.4 \times 10^8$  time steps when the population  $N \approx 45$ . The two peaks in the population histogram Figure 7a are the result of the emergence of coexisting short- and long-living cells. The left hand peak corresponds to the transient situation without long-living cells and the right hand peak is the sum of the contribution of the short-living cells (in shape identical to the left hand peak) and the fixed number of long-living cells. At this point in time, there are 17 cells with

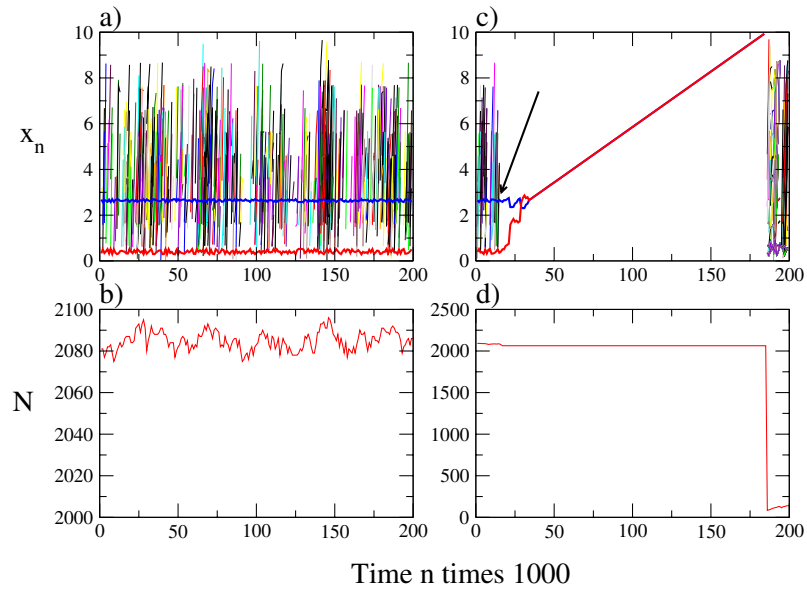


**Fig. 4.** Partially Ordered Phase with coexisting extremely-long- and short-living cells. The nonlinearity was set to  $K = 3.3$ . Graph a) depicts the situation after 62 million timesteps while c) shows the effect of setting the nonlinearity of the short-living cells to  $K = 0$  at the time point indicated by the arrow. Graphs b) and d) show the population strip charts corresponding to a) and c) respectively.

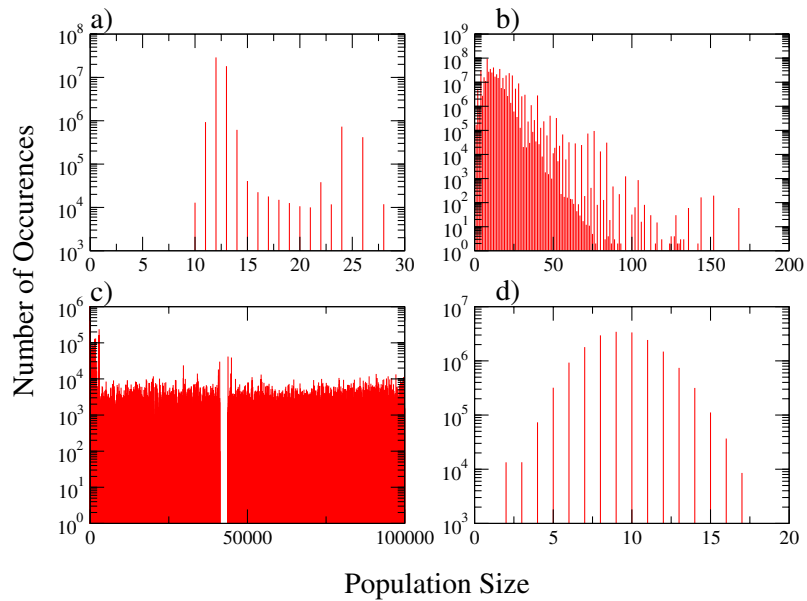


**Fig. 5.** Population size histograms. a)  $K = 1.0$  over  $5 \times 10^7$  time steps, b)  $K = 2.0$  over  $5 \times 10^8$  time steps, c)  $K = 3.1$  over  $9.6 \times 10^7$  time steps d)  $K = 3.6$  over  $1.8 \times 10^7$  time steps.

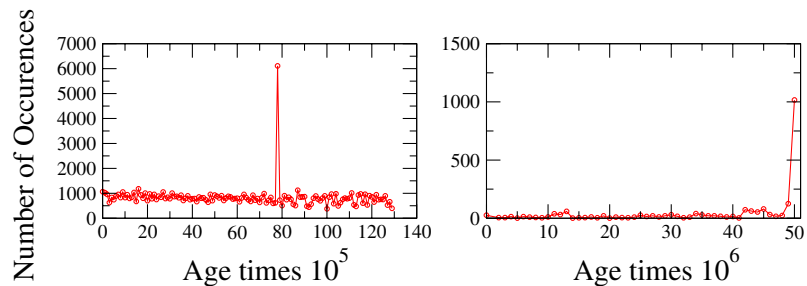


**Fig. 6.** Age histograms. a)  $K = 3.1$  (from the same data set as 5c),  $K = 3.3$  (from same the data set as 4a).

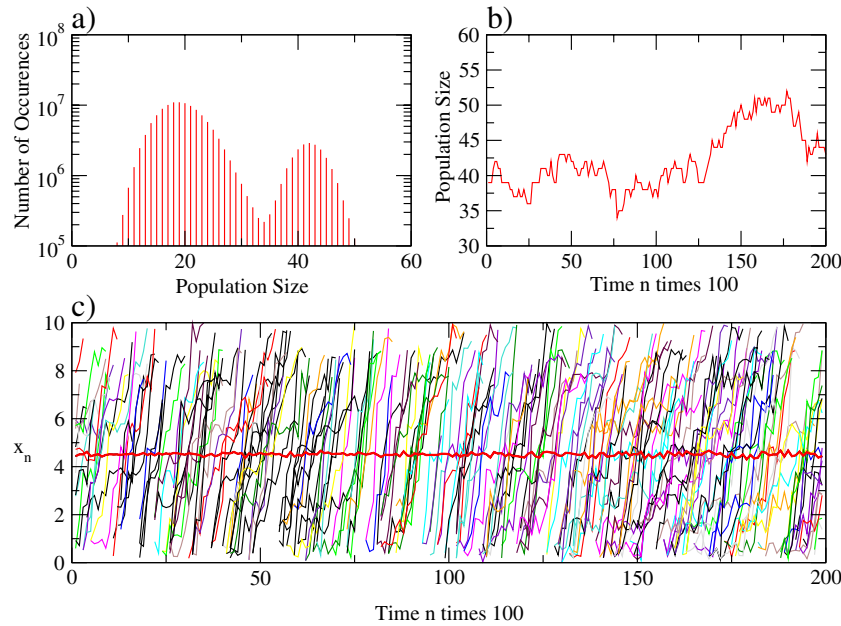


**Fig. 7.** Coexisting long- and short-living cells towards the end of the partially ordered phase. The nonlinearity is  $K = 3.45$  and the source is set to  $s = 0.1$ . Graph a) shows the population histogram after roughly  $1.4 \times 10^8$  timesteps. In b) the population-size strip chart is depicted while in c) the  $x$ -values of the population are shown.

ages ranging from 383 to 2560 timesteps, one cell with age 19185320 timesteps and 25 cells with ages ranging from 22202336 to 22788487 timesteps. Figure 7b shows the time evolution of the population size while c) depicts the cell states (plotted every 100<sup>th</sup> timestep). The thick line around  $x_n = 4.5$  corresponds to the long-lived cluster.

The introduction of a maximum life span would clearly have a drastic impact on the dynamics. For example if it were relatively short, the longer-living clusters which eventually attract the other cells to form a coherent cluster would not form thus decreasing the value of the nonlinearity  $K$  at which the partially ordered phase ends and the disordered phase starts.

For values of the source larger than  $s_c$ , the phases are summarized in Table 1.

#### 4 Sources smaller than $s_c$

Since an external source may not always be available, and since any finite source will eventually be exhausted by a rapidly growing population, it is of interest to investigate the dynamics of the model with  $s$  set to zero. The model then becomes

$$x_{n+1}^i = x_n^i + \frac{K}{2\pi} \sin(2\pi x_n^i) - \frac{1}{N} \sum_j \frac{K}{2\pi} \sin(2\pi x_n^j). \quad (4)$$

As is the case in equation (1), unless cells are removed from or added to the system, the sum of the cells  $\sum_j x_n^j$  is constant.

There are four main types of dynamical behavior with examples of three of them depicted in Figures 8–10: periodic, quasi-periodic and chaotic. For all figures, the first

one million timesteps were discarded and the initial value  $x_0$  of each cell was randomly set to a value between 5 and 6 in order for the cells to be able to grow or shrink somewhat without immediately splitting or dying. In all the figures, the left hand side depicts a strip-chart indicating the time evolution of  $x_n^i$  while the right hand side depicts the corresponding return map.

#### 4.1 Phase diagram

While the model in equation (4) allows for cells to be added and removed, this only happens for sufficiently large values of the nonlinearity  $K$ . Furthermore, the dynamics of the model is also dependent on the initial number of cells. A phase diagram for values of  $K$  ranging from 2 to 6 and for initial numbers of cells  $N^\circ$  ranging from 1 to 100 is depicted in Figure 11 (for  $N^\circ = 1$ ,  $x_0$  is a trivial fixed point).

The phase-diagram can roughly be divided into 5 parts although the boundaries may not be very sharp (for example, the transition from region III to IV/V is quite smooth):

- I *Periodic Orbits*: In this region all the attractors are periodic as a reflection of the underlying local map's periodicity. Figure 8 shows a typical orbit in this region. There is no division and death in this region.
- II *Quasi-periodic and Periodic Orbits*: There are two co-existent routes to chaos in a rather narrow region preceding region III. A typical example of a quasi-periodic trajectory is shown in Figure 9. As is the case with region I, there is no division and death.
- III *Chaotic, Quasi-periodic and Periodic Orbits*: This region is characterized by the coexistence of chaotic,

**Table 1.** Summary of the phases when  $s = 0.1$ .

Phase	Ordered Phase	Partially Ordered Phase	Desynchronized Phase
Clusters	1 or a few	Fluctuates between 1 and $N$	Approximately $N$
Population	Decreases from around 80 for $K = 0.1$ to around 6 for $K = 3.0$	Goes through 3 distinct stages: Desynchronized with a stable population, coexistence of short- and long-lived cells with (possibly) a slowly growing population, and ordered (coherent) with population collapse when the cells split.	Small with an average of around 40 for $K = 3.5$ to 2 for $K = 6.0$
$N_0$ dependence	None	None	When $N_0$ is very large (e.g. 1000), stable clusters can form
$K$	$0 < K \lesssim 3.0$	$3.0 \lesssim K \lesssim 3.45$	$3.45 \lesssim K \lesssim 6.5$
Notes	Up to $K \approx 1.6$ order is rather strictly coherent, afterwards splitting leads to slight fluctuations and possibly short term larger populations (giving a straight line in the semi-log plot of the population-size histogram).	After a rather long transient, the formation of coherent clusters was no longer observed and the system appeared to remain in a state of coexisting short- and long-living cells thus showing a clear differentiation of roles.	

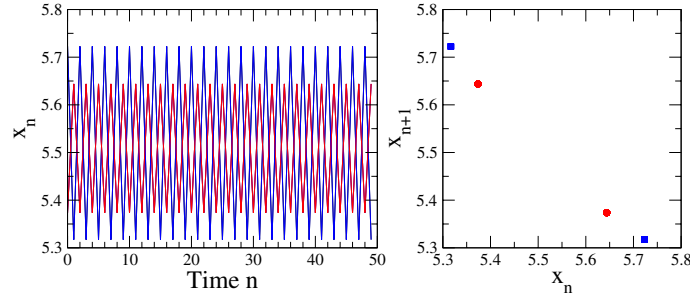


**Fig. 8.** Example of periodic motion. The nonlinearity is  $K = 2.5$  and the initial number of cells is  $N^\circ = 5$ . There are two period 2 clusters ( $N_1 = 3, N_2 = 2$ ) that are exactly out of phase with the smaller cluster having the larger amplitude.

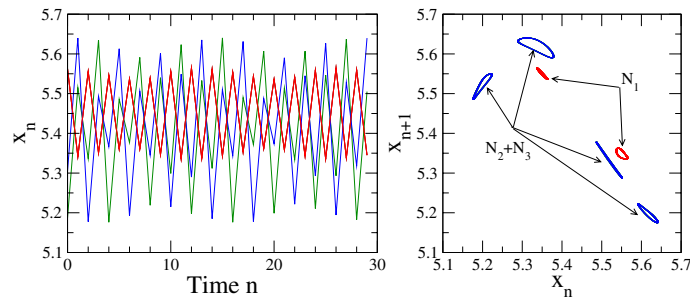


**Fig. 9.** Example of quasi-periodic motion. The nonlinearity is  $K = 2.64$  and the initial number of cells is  $N^\circ = 5$ . In this case there are three clusters ( $N_1 = 3, N_2 = 1, N_3 = 1$ ). The largest cluster has the smallest overall amplitude and its quasi-periodic motion is superimposed on a period 2 orbit. The two single cell clusters follow the same roughly period four quasi-periodic orbit but are out of phase.

quasi-periodic and periodic attractors. Since, as is the case for regions I and II, there is no division and death, the initial number of cells is conserved. For increasing nonlinearity and large values of  $N^\circ$ , the cluster distribution changes from roughly  $N_1 \approx N_2 \approx 0.5$  near region I to a somewhat more spread out distribution near region IV (cluster sizes ranging from 1 to 60 cells were observed for  $N = 100$ ).

Relatively the largest variety of cluster combinations was observed in the region marked as IIIa. It seems that an increase in the population has an adverse effect on the potential diversity in the system. Since as such, the attractors of  $N^\circ = 5$  are also attractors of  $N^\circ = 100$ , division and death should also occur to the right of the dashed line in region III. However, the stability may be different and indeed, in about 500

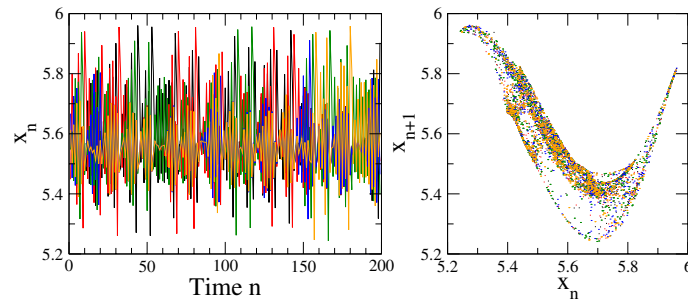


**Fig. 10.** Example of chaotic motion. The nonlinearity is  $K = 3$  and the initial number of cells is  $N^0 = 5$ . There are no clusters in this case and all the cells have different orbits.

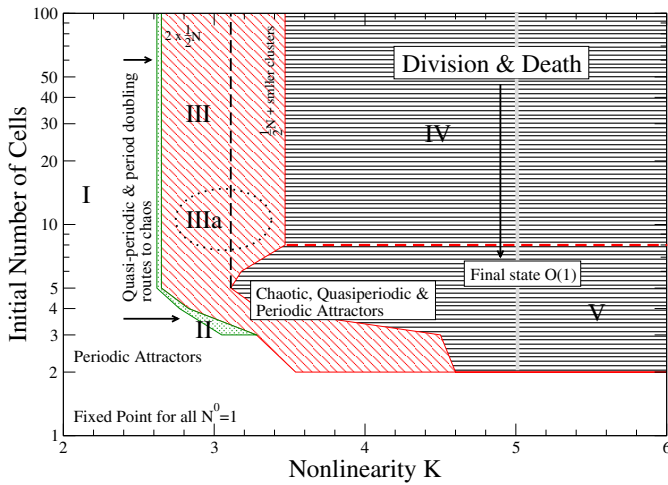


**Fig. 11.** Phase diagram for equation (4). There are five main regions: I – periodic attractors; II – quasi-periodic and periodic attractors; III – Chaotic, quasi-periodic and periodic attractors without cell death or birth. The dashed vertical line matches up with the left most dashed line and region IV should have the same attractors as the region V since attractors of  $N^0$  are also attractors of  $N^{100}$ . However, growth and death was not observed in this area indicating a different stability. The area marked as IIIa has relatively the largest variety of cluster combinations. IV – Feeder region through massive cell death for region V; V – Final state of region IV consisting of chaotic, quasi-periodic or periodic attractors.

trials not a single such event was found indicating that they are probably unstable.

IV *Cell Division and Death*: This region is basically a transient to region V. Large populations cannot be sustained and are rapidly reduced to order 1.

V *Chaotic, Quasi-periodic and Periodic Orbits & Final State of IV*: As in region III, periodic, quasi-periodic and chaotic attractors coexist in this region. During the transient, however, division and death are frequent. After the transient has died out, divisions and death do no longer occur and hence (with the current cell division scheme where both the daughters receive roughly half the parent cell's fractional  $x$ -value), none of the five regions allows for sustained life cycles.

Basically, the main types of phases as described by Kaneko [22] can be found in the the phase-diagram

Figure 11 as well. Even so, there are some quite significant differences between models (1) and (4), i.e. between the cases where  $s = 0$  and  $s \neq 0$ . A description of these differences is given below.

- *Coherent Phase*: For small  $K$ , there is a strong attraction to a coherent attractor. In the  $s \neq 0$  case, this attractor is not completely persistent however due to the incoherence that can be introduced when cells divide. Even for  $K = 0.1$ , e.g., coherence cannot be maintained for long times. Hence, as such, a strictly coherent phase does not exist when there is an external source term. When  $s = 0$ , the coherent attractor is the only attractor for small  $K$ . Since the global summation term and the local nonlinear term cancel out in Figure 4 when  $x^i$  is uniform, coherent attractors can be found for any value of  $K$  (in region V they are quite common, less so in region III).
- *Ordered Phase*: When  $s \neq 0$ , the ordered phase occurs for not too large values of the nonlinearity  $K$  and (when considering increasing  $K$ ) precedes the partially ordered phase. In the ordered phase, cells have quite a strong tendency to be synchronized but are not continually so. Generally (especially after the initial transients have died out) some desynchronization occurs when cells split. A characteristic feature of the ordered phase is that the final number of clusters is not dependent on the system size as long as it is not too small. This was also observed to be the case for the periodic and quasi-periodic orbits in regions II – V for the external source-free case where elements synchronize in a few clusters regardless of  $N^0$ .
- *Partially Ordered Phase*: In the partially ordered phase, system size independence of the cluster distribution is lost and cluster numbers can range from order 1 to  $N$ . For  $s \neq 0$ , this phase occurs between the ordered phase and the desynchronized phase which, in the terminology of the globally coupled logistic map [8], is an intermittent type of partially ordered phase since there are two temporal regimes, one in which many cells are desynchronized and one in which synchronization occurs towards the end of that temporal regime. In the  $s = 0$  case, however, once the cluster distribution of a periodic attractor has settled in, it will not change. Hence the type of partially ordered phase encountered is glassy, i.e. there is a coexistence basin-wise (rather



than time-wise) of many different cluster distributions. In the phase diagram, this type of dynamics can be found in region III for large  $N$  near the border to region IV.

- *Desynchronized Phase:* In the desynchronized phase, the behavior of the individual cells for  $s \neq 0$  is chaotic and the number of clusters is mostly equal to  $N$  (there can be some clustering for very short periods of time). Furthermore, the total number of cells remains quite small while cells continuously divide and die. For  $s = 0$ , the chaotic dynamics in regions III – V clearly form a desynchronized phase. Again, rather than being separated from the other phases time-wise or parameter-wise, the desynchronized phase of equation (4) coexists with the other phases and is separated from them basin-wise.

Roughly the differences can be summarized as follows. When  $s = 0$ , the four phases can overlap for the same value of  $K$  and hence have separate basins of attraction, while for  $s \neq 0$  the phases are the consequence of the value of  $K$  independent of the initial conditions.

## 4.2 Antiphase solutions

Due to the fact that the sum of the cells is constant as long as cells do not divide or die, all attractors consisting of two clusters are necessarily out of phase unless its a coherent attractor. Consequently, in the case of a chaotic attractor the orbit of one cluster exactly mirrors the orbit of the other cluster. An example of this is shown in Figure 12a where the two cells with the smaller values of  $x$  (the lower two lines) are out of phase as compared to the cell with the larger value of  $x$  (the upper line). Although the local dynamics is only determined by the fractional part, this behavior is not readily visible when plotting it as such as can be seen in Figure 12b. This type of attractor is not limited to three-cell systems, at  $K = 3.5$  with  $N^\circ = 5$  e.g. the same type of attractor with  $N_1 = 3, N_2 = 2$  was observed. In some cases, there is remnant chaos and as a consequence the composition of the cluster varies over time leading to a type of chaotic itinerancy. This is depicted in Figure 13 where the cell with the  $x$ -value in the middle first is in the same cluster as the cell with the lowest  $x$ -value and then switches to form a cluster with the cell that has the largest  $x$ -value. Since the switching is not very frequent, the strip-charts only show every 2000th time step (the figure depicts the system after around 2.5 million time steps. It was followed for another 100 million time steps and no qualitative change in the dynamics was observed).

A similar but qualitatively different behavior is shown in Figure 14. In this case, no clusters are formed but two cells closely follow one another in a shadowing-like manner with itinerant switches. In order to have some confidence in the genericity of this behavior, the attractor was again observed for one hundred million time steps with no signs of a qualitative change.

These attractors coexist with quasi-periodic and periodic attractors and also with chaotic attractors in which

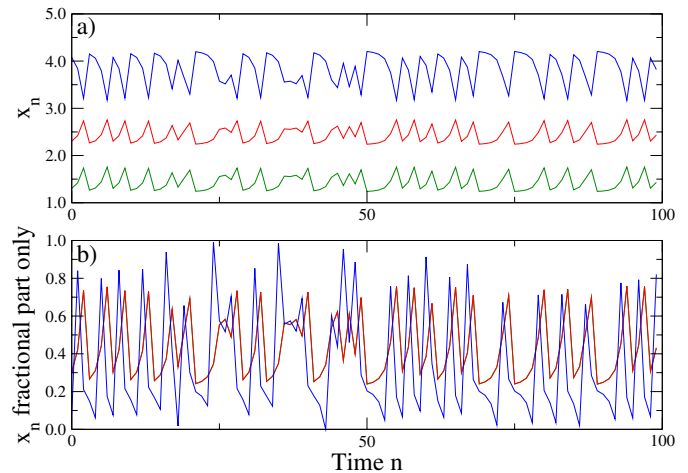


**Fig. 12.** Two-cluster antiphase solution. In a), the antiphase dynamics can clearly be seen, in b) which only depicts the dynamically relevant fractional part, however, this is not as obvious. The value of the nonlinearity is  $K = 4.5$  and the initial number of cells is 5. After the transient has died out and after discarding one million time steps, 2 clusters remain with  $N_1 = 2, N_2 = 1$ .

neither antiphase clustering nor shadowing-like behavior occurs (naturally sometimes the fractional parts of cells are very close, this proximity is however not sustained over longer time spans).

## 5 Dependence on settings

The most important parameter in equation (4) is clearly the local nonlinearity  $K$ . Nevertheless, other settings like the death and division conditions, the value of global coupling term etc. can possibly have a significant impact. In a certain sense these settings are somewhat similar to boundary conditions and it is therefore useful to know under what circumstances they need to be considered.

### 5.1 Death and division conditions

For  $s \neq 0$ , it was found that the division and death conditions generally do not qualitatively alter the dynamics of the system as long as they are integers and  $T_d < T_g$ . Mostly this is also the case for  $s = 0$  since as such the dynamics are determined by the fractional part of  $x_n^i$ . If  $T_g - T_d$  is too small however (e.g. 1 or 2), there is some impact. In regions I, II and III of the phase diagram, the death of a few cells (especially when  $N^\circ$  is large enough) is common without affecting the qualitative aspects (there is also some shift in the boundaries between the regions), and in regions III and IV, extinctions occur quite often for larger values of the nonlinearity  $K$ .

### 5.2 Effects of the sum

As the global coupling term  $S_n$  given in equation (2) is essential for the dynamics of the system and as this term

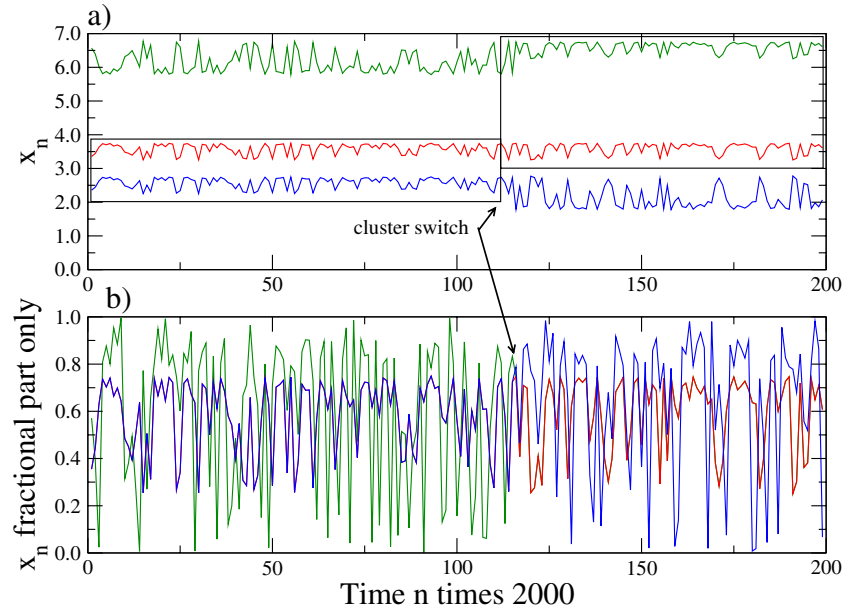


**Fig. 13.** Two-cluster antiphase solution with chaotic itinerancy. At first the middle cell forms a cluster with the lower cell. At the point in time indicated by the arrows it switches and forms a cluster with the upper cell. The strip-chart only shows every 2000th time step and hence covers a time span of four hundred thousand timesteps. The nonlinearity is  $K = 4.5$  and the initial number of cells was 4. After the transient has died out and after discarding one million timesteps, 2 clusters remain with  $N_1 = 2, N_2 = 1$ .

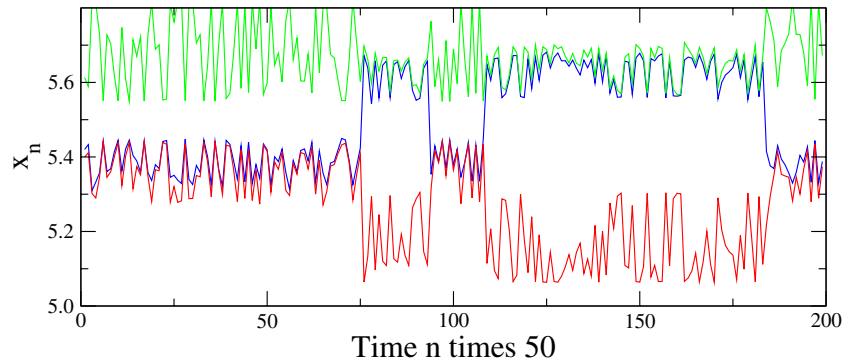


**Fig. 14.** Shadowing-like antiphase solution with chaotic itinerancy. The strip-chart only shows every 50th time step and hence covers a time span of forty thousand timesteps. The nonlinearity is  $K = 3.5$  and the initial number of cells was 3. After the transient has died out and after discarding one million timesteps, 3 single cell clusters remain with  $N_1 = N_2 = N_3 = 1$ .

remains constant unless cells die, it was investigated whether for a given  $S_0$  the basins of attraction for the various attractors mainly depend on this sum or not. The results are summarized in Table 2 and show that there is a clear correlation between the dominant dynamics and the initial value of the sum  $S_0$  for the medium strength nonlinearity in regions II and III. Not surprisingly, for small  $K$ , the periodic nature of the local map determines the state of the system while for larger  $K$ , the increased chaotic nature of the local map soon wipes out any memory of the initial condition.

The dependence of the dynamics on the initial sum is mostly limited to small system sizes. For example, for  $K = 3$  and  $N^\circ = 1000$ , 98 out of 100 runs ended on a periodic 2-cluster attractor with each cluster containing roughly half of the cells. The two remaining runs ended

on a chaotic attractor with one cluster containing roughly half the cells, one cluster roughly one quarter of the cells and some smaller clusters. Chaos was the strongest in the small clusters with the larger clusters being nearly periodic. Since all the attractors of the smaller initial cell populations are also attractors of the larger initial cell populations (though the stability of the attractors may change), the observed effects likely are due to a relative increase of the basin volume of the dominant attractor.

When a cell dies, its contribution to  $\sum_j x^j$  disappears in equation (1) and hence as well in equation (4). As already pointed out in [22], this is a particularity of the model. While the value of a cell may be small, due to the application of the (possibly highly nonlinear) local map, the effects can be quite significant (even when the system size is relatively large - e.g. around  $N = 100$ ).

**Table 2.** Summary of the dependence of the dynamics on  $S_0$ . The initial number of cells is  $N^\circ = 5$ . A clear correlation between  $S_0$  and the final dynamics is found for medium strength nonlinearities. m0.2 indicates that the results are modulo 0.2.

$K$	$S_0$	Dominant Dynamics
2	all	Independent of $S_0$
2.64	$\approx 0.10 - 0.14$ m0.2	$N_1 = 3, N_2 = 2$ periodic $N_1 = N$ coherent cluster
	$\approx 0.15 - 0.16$ m0.2	$N_1 = 3, N_{2,3} = 1$ periodic $N_1 = N$ coherent cluster
	$\approx 0.17 - 0.18$ m0.2	$N_1 = 3, N_{2,3} = 1$ Quasiperiodic $N_1 = N$ coherent cluster
	$\approx 0.19$ m0.2	$N_1 = 3, N_{2,3} = 1$ periodic $N_1 = 3, N_2 = 2$ periodic
	$\approx 0.2$ m0.2	$N_1 = 3, N_2 = 2$ periodic
	above mirrored to 0.3	mirrored to 0.3
3	$\approx 0.07 - 0.08$ m0.2	$N_1 = 3, N_2 = 2$ periodic $N_1 = N$ coherent
	$\approx 0.09 - 0.11$ m0.2	$N_1 = 3, N_{2,3} = 1$ periodic $N_1 = N$ coherent
	$\approx 0.12 - 0.13$ m0.2	$N_1 = 3, N_2 = 2$ periodic $N_1 = N$ coherent
	$\approx 0.14$ m0.2	$N_1 = 3, N_{2,3} = 1$ periodic $N_1 = N$ coherent
	$\approx 0.15$ m0.2	$N_1 = 3, N_2 = 2$ periodic $N_1 = N$ coherent
	$\approx 0.26$ m0.2	$N_1 = 3, N_{2,3} = 1$ quasiperiodic
	other values	$N_{1\dots k} = 1$ chaotic $N_1 = 3, N_2 = 2$ periodic
4	$\approx 0.08 - 0.12$ m0.2	$N_1 = N$ coherent cluster
	other values	Periodic and Chaotic Attractors
5	all	Independent of $S_0$
6	all	Independent of $S_0$

This is shown in Figure 15a where the thick solid line indicates the fractional part of the sum. In b) the sum is corrected by adding the the lost contribution of the dying cells back by distributing their last  $x$ -values evenly over the surviving cells as a one time source term. Clearly, the temporal dynamics of the system is drastically altered and consequently the relationship between initial conditions and selected final state. Overall, however, no new types of dynamics were observed.

### 5.3 Mutations

In order to find out whether there is some kind of evolutionary stable attractor in equation (4), it was investigated what the effects are of introducing mutation rates in the nonlinearity  $K$  when  $s = 0$ . First, the nonlinearity of a cell was mutated by a random value  $\in [-0.1, 0.1]$  when the age of the cell was modulus the inverse of the

temporal mutation rate. Second, the nonlinearity was adjusted for a newborn cell with a probability equal to the birth mutation rate again by changing  $K$  by a random value  $\in [-0.1, 0.1]$ . Lastly, both mutation schemes were applied simultaneously

In the cases where temporal mutations occur, for all the mutation rates ranging from 0.1 to 0.001, all the  $K$  and all  $N^\circ$  investigated, the result seemed to eventually be the same: A reduction of the population to a single cell (except for a few cases where the fractional parts of  $x$  were 0 and  $\frac{1}{2}$ ).

Clearly, the effects of a mutation rate at birth can only have an impact when the initial parameters lead to division. When it does have an impact, however, the results generally are as with the temporal mutation rate, a reduction of the population. The main reason for this is that the model seems to have a rather strong bias towards cell death and hence cell divisions are quite rare thus having little impact.

Somewhat related is the case where there is an initial random distribution of  $K$ . Again, for equation (4), the qualitative effects do not seem to be very large.

However, when  $s > s_c$ , the results of applying mutations are more interesting. With an initial random distribution of  $K$ , the population can split into two groups one of which rapidly grows and divides and one that lives for a long time (when  $K \in [2, 5]$ ). If the population is small, the stable group will be eliminated eventually (even though its life span is orders of magnitude larger than that of the other group). An example is shown in Figure 16 where one group remained stable for one million time steps while the other group divides roughly every 1700 time steps. The population fluctuates around 35 cells.

## 6 Division strategies

In order to keep the global sum constant, the division strategy chosen in [22] where the fraction above the division threshold  $T_g$  is divided among two daughter cells seems to be quite natural. There are, however, many other ways in which a cell in principle could divide and in order to find out whether the division strategy has a significant impact on the dynamics of the model, the effects of several other strategies are investigated below. These strategies are of course only relevant for regions where divisions occur, and only some representative values of  $K$  and  $N^\circ$  in areas IV and V were considered. All the attractors described in the phase diagram Figure 11 continue to exist since as such they are not dependent on cell division and death.

### 6.1 Strategy: fixed fraction

The local dynamics is entirely determined by the fractional part of  $x^i$  and one could hence argue that the magnitude of the fractional part is a key determining factor. Therefore, it may seem reasonable that when a cell divides, this attribute needs to be conserved and that the

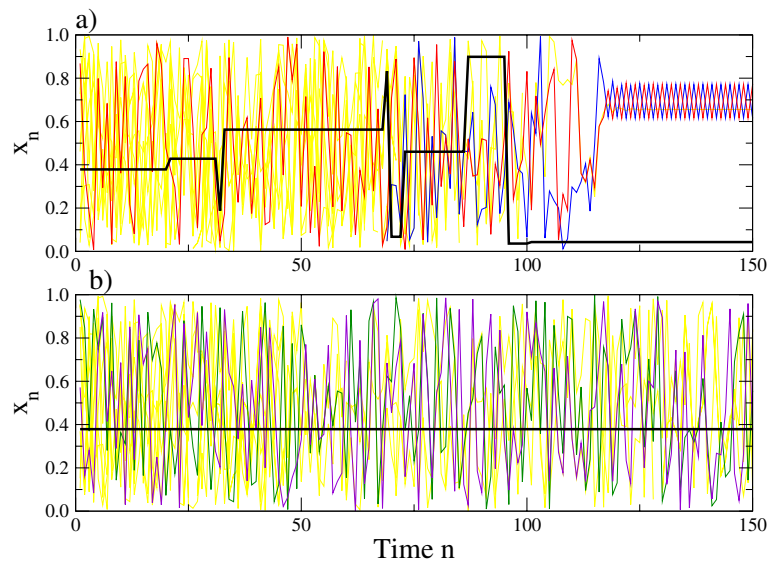


**Fig. 15.** For the model equation (1) as introduced and studied by Kaneko in reference [22], the sum indicated by the thick solid line can vary widely as can be seen in a). In b) the sum is corrected and fixed over time. The initial number of cells is  $N^\circ = 10$ , the nonlinearity is  $K = 6$  and the first 150 timesteps are shown. In a), a periodic attractor is reached after about 120 time steps.

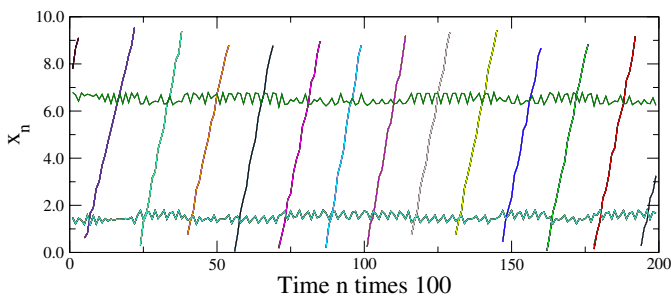


**Fig. 16.** The initial number of cells is  $N^\circ = 30$  and the initial nonlinearity is a random value  $K \in [2, 5]$ . The external source term is set to  $s = 0.1$ . As depicted, the population fluctuates around 35 cells with 18 rapidly growing cells that have  $K = 2.128075$ , 2 stable cells with that have  $K = 2.164091$  (the upper continuous line), and 16 stable cells that have  $K = 3.822824$  (the lower continuous line).

conservation of this attribute will have an impact on the overall dynamics of the population. This was not found to be the case, however. Although the global sum is not preserved under this strategy, similarly to when a cell dies, there seems to be little effect on the overall dynamics. It would be straightforward to correct for the change in the global sum but this inevitably would also change the phase of the cells and thus largely negate the purpose of this division scheme. Nevertheless, this was tried and again no significant impact was observed.

## 6.2 Strategy: half the parent

While the integer part of  $x^i$  is not relevant for the evaluation of the local map, it is nevertheless possible that the collective dynamics does have some dependence on it since

cells might move through several bands before stabilizing. From a conceptual point of view, one might further argue that if  $x^i$  stands for some generic physical quantity, giving the two daughters of a cell each half the contents of the parent cell is quite natural.

It was found that for  $N^\circ$  larger than around 8–12 cells in region V most initial conditions lead to a population explosion. It appears that this population explosion can be ascribed to the fact that the sum is not conserved when a cell dies. When the sum is corrected as in Section 5.2 similar population explosions were not observed.

## 6.3 Sustaining life cycles

With the combination of daughter cells receiving half the parent's  $x$ -value and the correction of the global sum when cells die, a significant qualitative difference as compared to the strategy where both the daughters receive half the fractional part, comes to light. When starting with  $N^\circ$  in region IV, the population no longer shrinks to region V but remains roughly around its initial value despite frequent divisions and deaths. Figure 17 shows a typical strip chart after around one million time steps have passed. The age of the oldest cell is only around 200 time steps. As can be seen, the cells are basically desynchronized growing and shrinking irregularly.

When starting from a certain initial population  $N^\circ$ , the population will generally grow slightly and then fluctuate randomly in a nearly Gaussian fashion until it falls onto an attractor. Figure 18 shows the population size histogram for the first one hundred thousand steps.

When increasing the initial population from  $N^\circ = 5$ , the transient time until reaching a periodic attractor at first increases nearly exponentially but then starts to decrease again when the  $N^\circ$  is large enough as can be seen in

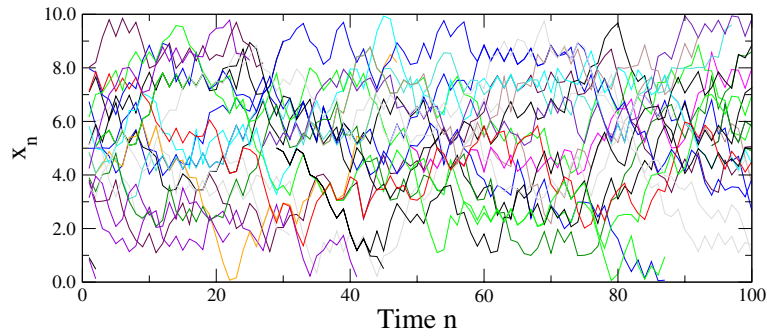


**Fig. 17.** Sustaining Life Cycles. The initial number of cells is  $N^\circ = 20$  and  $K = 6$ . For this figure the sum is kept constant when a cell dies and when a cell divides, both daughters receive half the parent's  $x$ -value plus or minus a small random value  $\delta < 10^{-5}$ . As always,  $T_d = 0$  and  $T_g = 10$ .

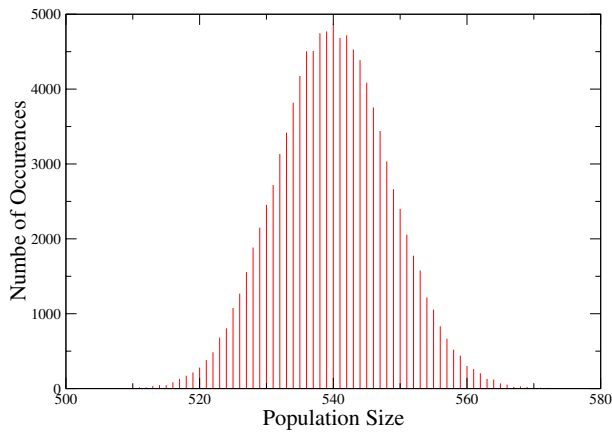


**Fig. 18.** Population histogram for the first  $10^5$  time steps. The sum is kept constant when a cell dies and when a cell divides, both daughters receive half the parent's  $x$ -value plus or minus a small random value of  $\delta < 10^{-5}$ . The initial number of cells is  $N^\circ = 500$  and  $K = 6$ .

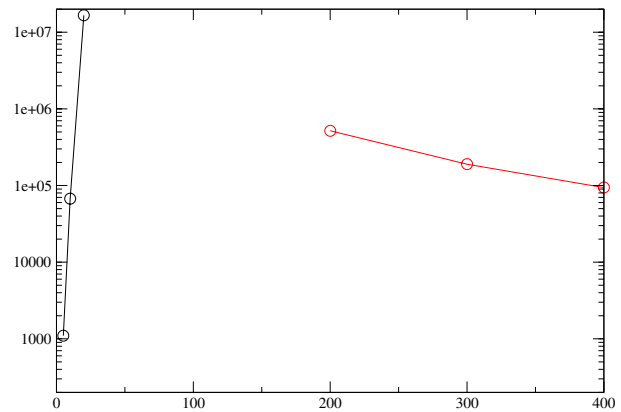


**Fig. 19.** The average transient time of 100 runs for the division strategy where the sum is kept constant where both daughters receive half the parent's  $x$  value plus or minus a small random value of  $1e-5$ . The nonlinearity is  $K = 6$ .

Figure 19. This seems to indicate that a periodic attractor can be reached when a system size independent minimum number of cells form a cluster. Since the average life span of a cell is only a few hundred time steps, the population goes through a very large number of life cycles.

When adding around 10% white noise, periodic attractors were no longer observed. Consequently, sustained life cycles are dynamically possible in the current model when the division strategy is such that both daughter cells receive about half of the parent cell's  $x$ -value combined with a sufficient amount of white noise.

## 7 Discussion and conclusion

The identification of models that display the dynamic characteristics of highly complex systems is of great importance for gaining insight into which aspects are essential and which aspects are peripheral. For systems with a fixed size, coupled map lattices have played a significant role in identifying universality classes and hence

extensions that include the addition and removal of elements seem to be both natural and relevant.

In this paper, one of the simplest coupled map lattices with growth and death is studied. When the source term is larger than a certain critical value it is found that differentiation of roles can occur in a parameter region of the partially ordered phase near the desynchronized phase after a fairly long transient. When the initial population is large and the nonlinearity not too small, it is furthermore shown that a previously employed cell division and death strategy leads to a strong decimation of the population without recurring life cycles when no external source is present. The existence of life cycles is, however, a key characteristic of biological systems and it's lack in the no-source scenario would diminish the value of the employed coupled map as a toy model, especially since the source term of the model does not have a one to one correspondence to an external source in a natural environment (after all the absence of the source term in the toy model neither necessarily leads to death nor to the absence of dynamics). It is found that the situation can be remedied by a natural modification of the division strategy combined with the preservation of the internal source and some white

noise leading to sustainable life cycles for a wide range of parameter values.

I would like to thank K. Kaneko for stimulating feedback and valuable suggestions. This work was partially supported by NUS grant No. R-144-000-111-112.

## References

1. K. Kaneko, Prog. Theor. Phys. **72**, 480 (1984)
2. K. Kaneko, Physica D **34**, 1 (1989)
3. F.H. Willeboordse, Chaos, Solitons and Fractals **2**, 609 (1992)
4. F.H. Willeboordse, Chaos **4**, 89 (1994)
5. J.P. Crutchfield, K. Kaneko, *Directions in Chaos* (World Scientific, Singapore, 1987)
6. F.H. Willeboordse, Phys. Rev. E **47**, 1419 (1993)
7. S.P. Kuznetsov, in *Theory and Applications of Coupled Map Lattices*, edited by K. Kaneko (Wiley, New York, 1993), p. 50
8. K. Kaneko, Physica D **41**, 137 (1990)
9. Y. Kuramoto, H. Nakao, Phys. Rev. Lett. **76**, 4352 (1996)
10. A. Pikovsky, M. Rosenblum, J. Kurths, Europhys. Lett. **34**, 165 (1996)
11. O. Popovych, A. Pikovsky, Y. Maistrenko, Physica D **168**, 106 (2002)
12. N.B. Ouchi, K. Kaneko, Chaos **10**, 359 (2000)
13. F.H. Willeboordse, Phys. Rev. E. **65**, 026202 (2002)
14. F.H. Willeboordse, Chaos **13**, 533 (2003)
15. P.G. Lind, J. Corte-Real, J.A.C. Gallas, Phys. Rev. E **69**, 026209 (2004)
16. E. Ko, T. Yomo, I. Urabe, Physica D **75**, 81 (1994)
17. T.S. Gardner, C.R. Cantor, J.J. Collins, Nature **403**, 339 (2000)
18. C.C. Guet, M.B. Elowitz, W. Hsing, S. Leibler, Science **296**, 1466 (2002)
19. M.B. Elowitz, S. Leibler, Nature **403**, 335 (2000)
20. C.H. Yuh, H. Bolouri, E.H. Davidson, Science **279**, 1896 (1998)
21. K. Kaneko, T. Yomo, J. Theor. Biol. **199**, 243 (1999)
22. K. Kaneko, Physica D **103**, 505 (1997)